Tomography-like Approach for Analysing Colour Auroral Images

Noora Partamies[1], Björn Gustavsson[2], Laureline Sangalli[3], Mikko Syrjäsuo[4],
Eric Donovan[5], Martin Connors[6] and Dan Charrois[7]

[1] Finnish Meteorological Institute, P.O. Box 503, FIN-00101, Helsinki, Finland
[2] University of Southampton, UK
[3] Royal Military College of Canada, Kingston, Ontario, Canada
[4] Aalto University, Espoo, Finland
[5] University of Calgary, Calgary, Alberta, Canada
[6] University of Alberta, Athabasta, Alberta, Canada
[7] Syzygy Research & Technology, Legal, Alberta, Canada
[*] Corresponding author, e-mail: noora.partamies@fmi

Abstract

We report the first attempt to use tomography-like reconstructions tool with colour auroral images. A colour camera imaging system (DAISY) was designed for studying the altitude profiles of the aurora, but the wide-band colour image data have not been tested for tomography-like analysis before. DAISY campaign measurements provide a large number of simultaneous auroral images with clear skies and aurora at two stations. We used images with simple, well-defined auroral structures and clear maximum in the emission intensity to examine whether images without narrow-band optical filters can be used for tomographic reconstructions. Our results suggest that the green line emission, which is the strongest auroral emission at λ = 557.7 nm, can be well-reconstructed with meaningful peak emission altitudes and horizontal scales even from the wide-band colour images. Fainter emissions at red (λ = 630.0 nm) and blue (λ = 427.8 nm) wavelengths could not be sufficiently separated from the dominant green spectral line due to the properties of the colour matrix of the CCD.

Key words: colour auroral imaging, tomography, ionosphere

1. Introduction

Auroral tomography has evolved from earlier applications, such as the stereoscopic triangulation (*Vegard and Krogness*, 1920), two-dimensional fitting of absolute intensities of photometer measurements (*Romick and Belon*, 1967) and satellite radio tomography (*Austen et al.*, 1986). The idea of the method is to utilise data from several auroral cameras at different locations to view the same auroral feature from different angles. From these observations either a two-dimensional (latitude vs. altitude) map or a three-dimensional reconstruction of the volume emission rate can be inferred by using e.g. stochastic inversion (*Nygrén et al.*, 1996) or iterative inversion methods (*Frey et al.*, 1998; *Gustavsson*, 1998). The horizontal resolution of the tomography results and the size of the common volume in the ionosphere depends on the number of imaging

stations and their separation as well as the pixel resolution of the images and the field-of-views (FoV) of the cameras. Favourable distances between the cameras vary from 20 km to 200 km (*Frey et al.*, 1996a,b), although shorter distances have been used to estimate altitudes of auroral fine-structures (*Ivchenko et al.*, 2005). The reliability of the result is also affected by the thickness and the width of the auroral structure, separation between structures (e.g. multiple arcs) and the location and orientation of the aurora with respect to the imagers. Usually a priori information must be included in the inversion procedure. In case of the stochastic inversion it is embedded in the regularisation, while in the iterative methods this information comes into play when choosing the start guess profile for the volume emission rate and the stop criteria for the iteration. An iterative approach is what is being utilised in this study.

The challenge in the auroral tomography is to estimate the 3D distribution of auroral volume emission rates from a limited number of images spanning an incomplete set of viewing angles. When multiple auroral structures are viewed from too few directions, it is not always possible to resolve them all and determine to what extent each structure contributes to the image intensities. This is why we call this a tomography-like method rather than tomography. The more viewing directions (camera stations) are available the more stable the reconstruction becomes. When the emission curtains extending along the magnetic field appear as separate arcs it is possible to estimate the altitude and horizontal distribution of volume emission rates. Using image data filtered for one emission wavelength (the traditional way of doing auroral tomography) may help with determining a more plausible starting guess for the altitude profile of the emission. The motivation for tomographic approaches in the auroral physics is to study the altitude (magnetic field-aligned) profiles of auroral emissions. Information on different emission lines can be used to study the evolution of the characteristic energy of the incoming particles. Other than point measurements from rockets and incoherent scatter radars, there are very few alternatives to determine even just the peak emission altitude. Thus, more quantitative methods for ground-based optical data are very important.

Colour imaging of the aurora started in early 2000 as reported by *Syrjäsuo et al.* (2005). Most colour cameras incorporate wide angle or all-sky optics and have mainly been used for monitoring the occurrence of the aurora. However, it has been shown that the intensity of the three most dominant auroral emissions ($\lambda = [630.0, 557.7, 427.8]$ nm) can be estimated from colour images by comparing image intensities with simultaneous observations made with an intensity calibrated optical instrument (such as a photometer or a camera with filters) which has an overlapping FoV with negligible light pollution (*Partamies et al.*, 2007). Thus, information on the most dominant auroral emissions can be deduced from colour data.

Dense Array Imaging SYstem (DAISY, *Partamies et al.* (2008, 2010)) consists of three colour cameras with FoVs of 20°, 90° and 90°. The system was designed for auroral optical campaigns to study the altitude profiles of auroral emissions. The system is also transportable facilitating campaign measurements in different locations with different support instrumentation. For tomography-like applications the system is run with the narrowest FoV camera pointing in the direction of the local magnetic field, and the larg-

er FoV imagers viewing the same ionospheric column from the northern and southern side, respectively.

DAISY uses three colour components (red, green and blue) to describe the perceived colour of the spectrum recorded by the camera. This is also the most common technique used in consumer digital cameras. Figure 1 illustrates the relative responses of these three colour channels. However, as each channel has a wide response range contributing to a single integrated intensity value, details such as individual auroral emission lines cannot be distinguished in the data. Unfortunately, this integrating property also applies to other light sources such as street lights: the contribution of light pollution cannot be determined with certainty. A dark observation site, however, can provide a sufficiently good auroral light to background illumination ratio. A more detailed technical description of DAISY can be found in *Partamies et al.* (2008).

In this paper, we describe the first tomography results of the DAISY images. To the best of our knowledge this is the first attempt for auroral tomography on colour images.
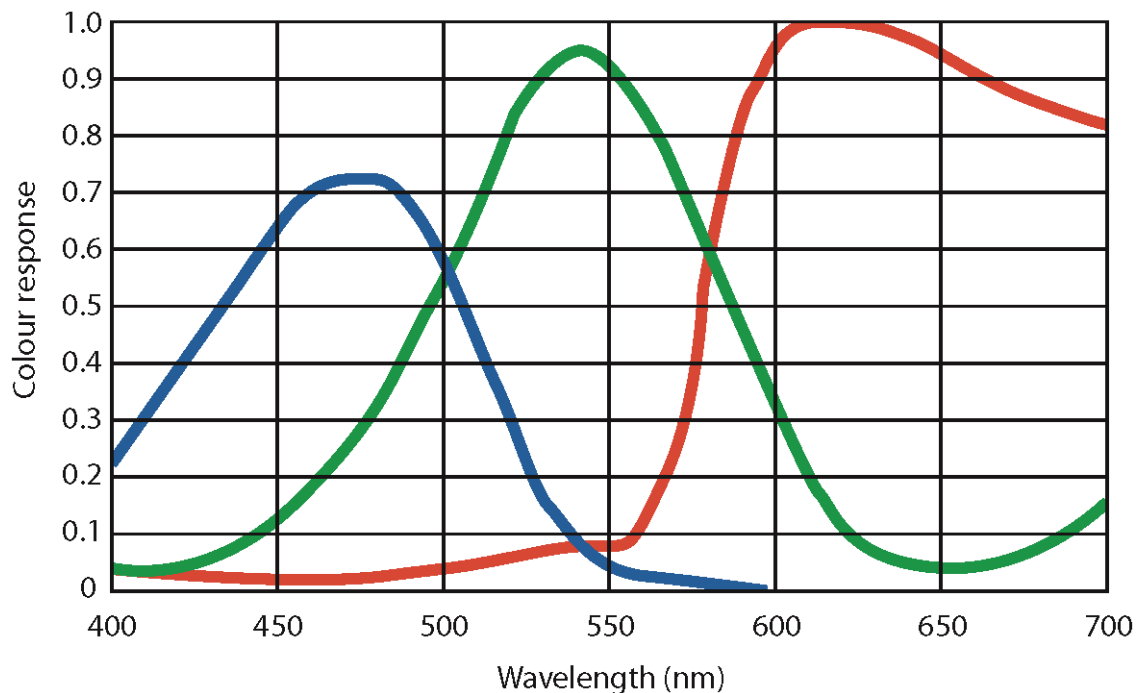

Fig. 1. Relative colour responses of the wide-band blue, green and red (maxima left to right) channel of the Bayer colour matrix. These curves are reconstructed from the data sheet provided by the manufacturer, and their maxima are close to the three main emission lines of the aurora (λ = [427.8, 557.7, 630.0] nm).

2. *Tomography of colour auroral images*

For the DAISY measuring campaign in Alberta, Canada, in March 2007, the DAISY cameras were deployed in Legal (53.95°N, 246.41°E), Athabasca (54.71°N, 246.69°E) and Calling Lake (55.18°N, 246.77°E). The middle station in Athabasca was equipped with the narrowest 20° FoV camera pointing to the magnetic zenith with a

zenith angle of about 13°. During a two-week campaign, no aurora was recorded from all three stations in good weather conditions. The middle and south stations were operated for another two weeks and obtained good auroral data, which will be analysed here. The distance to the south station in Legal from Athabasca is about 86 km. The 90°FoV in Legal was tilted about 30° northward to view the ionospheric volume above the middle station.

We used an Auroral Image Data Analysis software package AIDA-tools for tomography-like application (*Gustavsson*, 2002, 2008) that has been designed for Swedish Auroral Large Imaging System (ALIS) network (*Brändström*, 2003). The pointing direction of each pixel was determined using the known locations of stars that are visible in the auroral images. The tomographic reconstruction then gives a three-dimensional volume emission rate in the common volume of the two imagers.
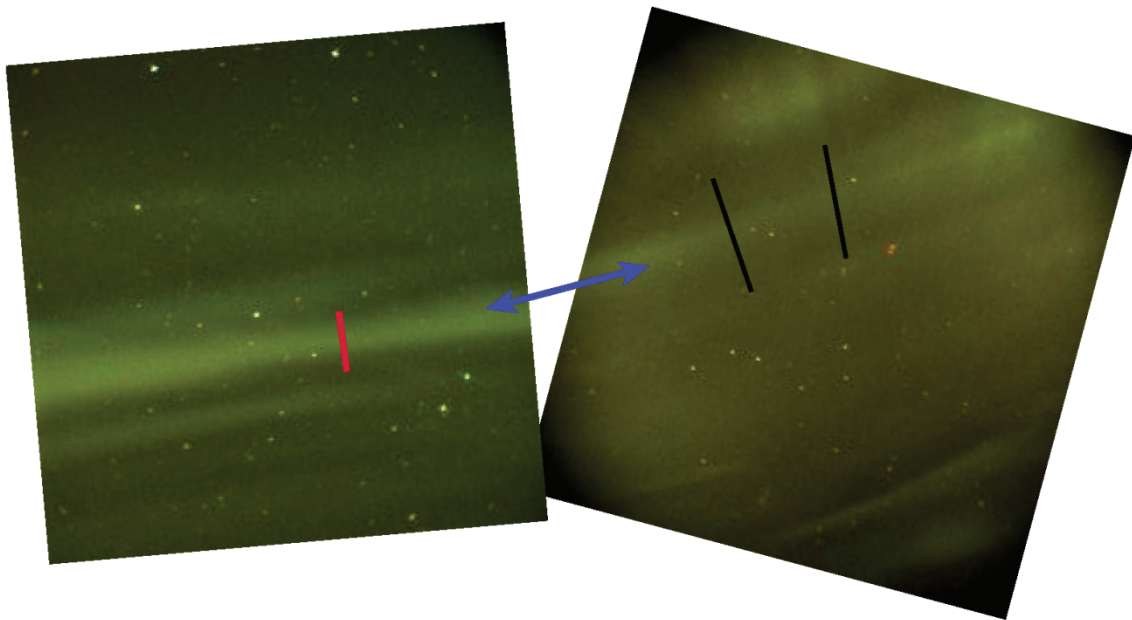

Fig. 2. An example of simultaneous full colour images from the middle station in Athabasca (left) and south station in Legal (right), with FoVs of 20° and 90° respectively. North is to the top. The images have been taken at 06:02:36 UT on 24 March, 2007 with an exposure of 4 seconds. The brightest stars seen in the images have been used to determine the camera pointing. The reconstructed volume emission rate of these images is plotted in the following figure. The red line marks the cross-section, for which the brightness profiles are plotted in Figure 4. The reconstruction slice also closely follows the same cross-section.The blue arrow indicates the arc of interest in both FoVs, and black lines mark the edges of the projection of the Athabasca FoV on Legal image.

The data used in this study was recorded on 24 March, 2007. Driven by a strongly negative interplanetary magnetic field (IMF $Bz < 0$) for the whole day, the geomagnetic activity reached storm conditions with a Dst index minimum of -72 nT at 09 UT. Auroral activity in the Canadian sector around magnetic midnight lasted for several hours with multiple intensifications and a vast variety of different structures including both diffuse and discrete precipitation. Figure 2 consists of a pair of simultaneous auroral images from the middle station in Athabasca (left) and southern station in Legal (right) converted to full colour. We searched for simple auroral structures (arcs) with a clear max-

imum in the emission intensity in order to accurately determine the altitude of the peak emission. An altitude for the widest and brightest auroral arc in the image on the left (marked by the red line) as estimated by triangulation (*Sangalli et al.*, 2011) was 105 km. The blue arrow in Figure 2 points to the corresponding structure in both images. The edges of the Athabasca FoV have been projected to the larger FoV of the Legal image on the right (black lines).

A north-south slice of the tomographic reconstruction of the same image pair is plotted on the left panel in Figure 3. North is to the right, and the location of the middle station is at 0 km on the X axis. The colour-coding illustrates the volume emission rate. Sharp skewed edges in the volume emission rate are artefacts of the edges of the camera FoVs.The main auroral arc in the reconstruction volume (located at between -20 and -15 km) has been sliced horizontally to find the altitude of the peak volume emission rate, which appeared at about 100 km in agreement with the triangulation result. Lowering edge of the volume emission to the right is an effect of the artificial dark red region, which is the far end of the intersecting FoVs. In the panel on the right, we show a height profile of the reconstructed volume emission rate through the main auroral arc.
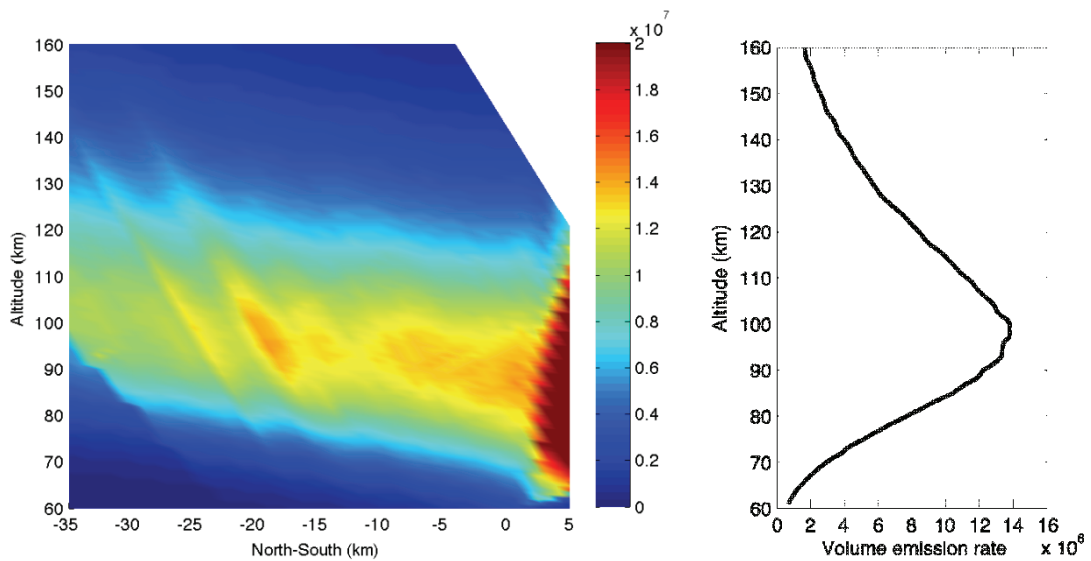

Fig. 3. Left: A north-south slice through the reconstruction volume shows the vertical profile of the auroral arc presented by images in the previous figure. Colour-coding describes the volume emission rate (photons/m^{3}s), which corresponds to the measured emission intensity. The sharp skewed colour edges on the left and right in the plot are artefacts produced by the edges of the FoVs. The white upper right corner of the plot is the edge of the reconstruction region, and the dark red lower right corner is an artefact from the FoV edges. The middle station is located at 0 km looking along the magnetic field (13 degrees zenith angle southward). Negative values are to the south of Athabasca. Right: A volume emission rate height profile through the main auroral arc.

The reconstruction volume consists of 1 km full-width half-maximum (FWHM) cos^2-shaped basis functions (*Rydesäter and Gustavsson*, 2001) that overlap with their nearest neighbours in a grid that is skewed to be parallel to the magnetic field and horizontal plane. The grid covers altitudes from 60 to 180 km. In the horizontal direction the size of reconstruction volume is 110×110 km and it is centered with the common vol-

ume of the camera FoVs at the altitude of 110 km. We use Multiplicative Albegraic Reconstruction Technique (MART, *Herman et al.* (1976)) for six iterations. This is a fast technique, which was tested to re-produce the auroral structures very well as compared to other, more time-consuming iterative methods or a larger number of iterations. The starting guess for the height distribution of the volume emission rate is a Chapman profile with the maximum altitude given by triangulation and the FWHM of the profile assumed to be 20 km. This is important because the result is dependent on the peak altitude and FWHM of the Chapman profile. If the viewing directions could be added (in our case, images from the third DAISY station), the result would be less sensitive to these start guess values. For the number of iterations larger than six the changes in the result were negligible. The overestimate of the far edge volume emission rate (the dark red region on the right) of the reconstruction region is due to the fact that for those directions the line-of-sight intersection with the reconstruction volume is short. This results in significant contribution to the total intensity from the region outside the reconstruction volume to be compressed into that short intersection region leading to these artefacts. Within the reconstruction volume the relative intensities of the two cameras have been inter-calibrated, and thus, the excess luminosity accumulates in the far corner outside the reconstruction volume. The reproduced signatures are reliable in the regions with overlapping fields-of-view where auroral emission dominates the background luminosity, i.e. in case of a strong signal, despite the edge artefacts. The tomography algorithm itself has been tested to work well on the auroral image data (*Gustavsson*, 2002).

As an example, a horizontal cross-section of the auroral arc in the reconstruction (between -20 and -15 km) is plotted in Figure 4 (black). The altitude of of the slice is 105 km . This profile has been interpolated from the reconstruction base function intensities with a $\cos^2$-shaped point-spread function. We compare it with the brightness profile of the arc in the original image (red line in left panel of Figure 2) projected to the altitude of 105 km. The blue curve in Figure 4 is the Gaussian profile fitted to the raw data in the direction perpendicular to the auroral arc, which is approximately along the magnetic meridian and gives the shortest distance across the arc. Both curves have been normalised and the background has been subtracted. We chose the height for this comparison to be the maximum emission height suggested by the real data rather than the maximum volume emission rate height of the reconstruction. While the pixel resolution of the colour image is about 100 m, the distance across the arc in Figure 4 is about 50 m per unit step after fitting and interpolating. The width of the auroral structure in the tomography result is in agreement with the observed brightness profile, both suggesting a FWHM of about 2 km.
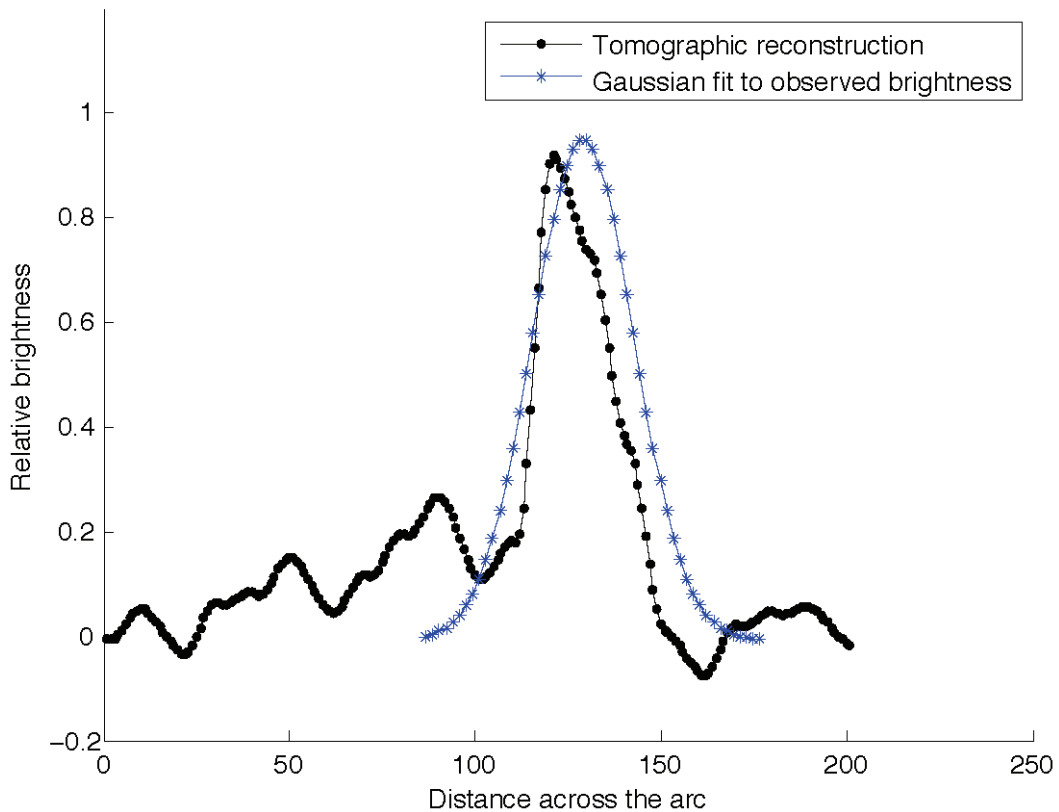
Fig. 4. Comparison of the arc cross-section in the reconstruction (black) and in the Gaussian fitted brightness (blue). Both profiles have been de-trended and normalised. The profiles describe the arc between -20 km and -15 km in Figure 3. Neighbouring structures have been cropped out for fitting a single Gaussian curve. The distance across the arc is in data points and one point corresponds to about 50 m.

We also examined the altitude variation along thin well-defined auroral arcs by triangulating 12 structures and 8–15 points along each form. This showed a peak emission altitude variation along the arcs of 2–4 km within the 20° FoV that corresponds to about 36 km at the height of 100 km. For all studied auroral structures the average altitude of the maximum emission varied between about 100–105 km.

3.   Summary and conclusions

The tomographic reconstruction using the wide-band green channel of DAISY colour auroral images produced promising results. As seen from the example images in Figure 2 the stars are clearly visible allowing good geometric calibration and accurate pointing of the cameras. The reconstructed auroral structure in Figure 3 shows the maximum altitude of about 100 km which agrees with the height of 105 km obtained by triangulation. This is somewhat lower than the typical assumption of 110 km for the auroral green emission maximum, but completely plausible during active conditions. Further spectral information is needed to estimate the precipitation energy. The width of the reconstructed sample arc is about 2 km, which is in agreement with the FWHM of the brightness (Fig. 4).

Because the brightness profiles of the raw data contain some measurement noise, we use the Gaussian fit to compare the observed width to the reconstructed one. Both curves behave smoothly and suggest slightly wider structures than what the images show, because we fit raw (unprocessed) brightness values. The width of the reconstructed arc is narrower then the brightness curve because the tomography-like reconstruction untangles the vertical-to-horizontal spreading of the structure as it is projected onto the image plane. The size of the reconstruction basis function (1 km) limits the scale of the auroral features that may be reliably resolved by the method.

Of course, the inversion can be done for smaller basis functions but it then requires much more computer time and memory than what an average laptop has in 2011. This could be compensated by shrinking the reconstruction volume, but this would lead to edge effects closer to, or even within the common volume. Thus, we chose to use a combination of a larger common volume and wider basis functions that is faster to process and requires less manual fine-tuning.

The colour matrix integrated on the top of the CCD detector absorbs some of the incoming light. This results in a somewhat less sensitive instrument as compared to an unfiltered imager. As seen from the sample images (Fig. 2) the green emission is dominant. As illustrated in Figure 1, all the DAISY colour channels include the entire visual wavelength range and thus, are so wide compared to the auroral emission lines that the intense green light leaks into the red and blue channels as well. So far, we have no DAISY data that would show a distinct blue or red auroral emission, so the tomography-like reconstruction has only been tested for the wide-band colour channel maximising around the auroral green wavelength. Green auroral tomography is likely to be the only one working for most cases. The red emission is often so structure-less that determining the maximum emission altitude for the start guess with a reasonable accuracy can be very challenging. Furthermore, both blue and red emissions may appear so weak that in the DAISY colour data they may not be detected at all if any green aurora is present simultaneously in the same region. Our results further suggest that tomography-like approach could also be used for panchromatic (whitelight) imager data to study the altitude profile of the green emission, but without any spectral information.

DAISY was designed and built as a feasibility study for more advanced use of low-cost wide-band auroral imaging. To answer the science questions of existence of 1 km wide auroral structures and emission profile studies, intensity calibration was not necessary and has not been performed. A recently published method by *Sigernes et al.* (2008) would allow intensity calibration for this type of an imager, and consequently, the emission intensity and volume emission rate values would become more reliable.

References

Austen, J.R., S.J. Franke, C.H. Liu, and K.C. Yeh, 1986. Application of computerized tomography techniques to ionospheric research, in *Radio beacon contribution to the study of ionisation and dynamics of the ionosphere and corrections to geodesy*, Edited by A. Tauriainen, University of Oulu, Oulu, Finland, Part 1, 25–35.

Brändström, U., 2003. The Auroral Large Imaging System – Design, operation and scientific results, *IRF Sci. Rep.*, 279,
http://www.irf.se/Publications/IRFreport279.pdf

Frey, H.U., S. Frey, B.S. Lanchester, and M. Kosch, 1998. Optical tomography of the aurora and EISCAT, *Ann. Geophys.*, **16**, 1332–1342.

Frey, S., H.U. Frey, D.J. Carr, O.H. Bauer, and G. Haerendel, 1996a. Auroral emission profiles extracted from three-dimensional reconstructed arcs, *J. Geophys. Res.*, **101**, 21731–21741.

Frey, H.U., S. Frey, O.H. Bauer, and G. Haerendel, 1996b. Three-dimensional reconstruction of the auroral arc emission from stereoscopic optical observations, *SPIE Proc.*, **2827**, 142–149.

Gustavsson, B., 1998. Tomographic inversion for ALIS noise and resolution, *J. Geophys. Res.*, **103**, 26621–26632.

Gustavsson, B., 2002. Three dimensional imaging of aurora and airglow, PhD thesis, Swedish Institute for Space Physics, http://www.irf.se/ bjorn/thesis/thesis.html.

Gustavsson, B., M.J. Kosch, A. Senior, A.J. Kavanagh, B.U.E. Brändström, and E. M. Blixt, 2008. Combined EISCAT radar and optical multispectral and tomographic observations of black aurora, *J. Geophys. Res.*, **113**, A06308, doi:10.1029/2007JA012999.

Herman, G.T. and A. Lent, 1976. Iterative reconstruction algorithms, *Compt. Biol. Med.*, **6**, 273–294.

Ivchenko, N., E.M. Blixt, and B.S. Lanchester, 2005. Multispectral observations of auroral rays and curls, *Geophys. Res. Lett.*, **32**, L18106, doi:10.1029/2005GL022650.

Nygrén, T., M. Markkanen, M. Lehtinen, and K. Kaila, 1996. Application of stochastic inversion in auroral tomography, *Ann. Geophys.*, **14**, 1124–1133.

Partamies, N., M. Syrjäsuo, E. Donovan, and D. Knudsen, 2008. Dense Array Imaging SYstem prototype observations of missing auroral scale sizes, in Proceedings of the 33rd Annual Meeting on Atmospheric Studies by Optical Methods, *IRF Sci. Rep.*, **292**, 95–101, http://www.irf.se/publications/proc33AMfiles/partamies-etal.pdf.

Partamies, N., M. Syrjäsuo, E. Donovan, M. Connors, D. Charrois, D. Knudsen, and Z. Kryzanowsky, 2010. Observations of the auroral width spectrum at kilometre-scale size, *Ann. Geophys.*, **28**, 711–718.

Partamies, N., M. Syrjäsuo and E. Donovan, 2007. Using colour in auroral imaging, *Canadian Journal of Physics*, **85**, 101–109.

Romick, G.J., and A.E. Belon, 1967. The spatial variation of auroral luminosity– II, *Planet. Space Sci.*, **15**, 1695–1716.

Rydesäter, P. and B. Gustavsson, 2001. Investigation of smooth basis functions and an approximated projection algorithm for faster tomography, *Imaging Systems and Technology*, **11**, 347–354, DOI: 10.1002/ima.1019.

Sangalli L., B. Gustavsson, N. Partamies and K. Kauristie, 2011. Estimating the peak auroral emission altitude from all-sky images, in proceedings of The 37th Annual European Meeting on Atmospheric Studies by Optical Methods, *Óptica Pura y Aplicada*, **34**, 593–598.

Sigernes, F., M. Dyrland, N. Peters, D.A. Lorentzen, T. Svenøe, K. Heia, S. Chernouss, C.S. Deehr, and M. Kosch, 2008. The absolute sensitivity of digital colour cameras, *Optics Express*, **17**, No. 22, 20211–20220.

Syrjäsuo, M. T., B. J. Jackel, E. F. Donovan, T. S. Trondsen, and M. Greffen, 2005. Low-cost multi-band ground-based imaging of the aurora, in Proceedings of SPIE, 5901, Solar Physics and Space Weather Instrumentation, edited by Silvano Fineschi, Rodney A. Viereck, 59010F1–11.

Vegard, L. and O. Krogness, 1920. The position in space of the aurora polaris, Geofysiske publikationer, 1–170, A. W. Brøggers Boktrykkeri A/S.